False Detections in an Optical Coding-Based PON Monitoring Scheme

Manuel P. Fernández, Pablo A. Costanzo Caso, *Member*, *IEEE*, Laureano A. Bulus Rossini.

***Abstract*— We address the issue of false detections in an optical coding-based PON monitoring scheme. An analytical expression for the average number of false detections is derived and the system performance in terms of false detections is evaluated. We show that a feasible, low-cost scheme can monitor a large number of users with less than one false detection per user even in high-density PONs.**

***Index Terms*— PON monitoring, code division multiplexing, false detections, network discovery algorithm**

I. Introduction

AUTOMATICALLY detecting and locating the branch in which a fault (e.g. a fiber break) has occurred in a Passive Optical Network (PON) reduces operating expenditures (OPEX) and minimizes the mean down time (MDT).

Optical Time Domain Reflectometry (OTDR) presents severe limitations when applied in branched networks [1]. Hence, some schemes based on optical code division multiplexing (OCDM), that place passive encoders at the end of each drop fiber, have been proposed [2]-[5] and demonstrated [6]-[7] to overcome this issue. In the central office (CO), a network discovery algorithm needs to detect all codes in the received signal.

Interference between codes may cause false detections. To this respect, if the network discovery algorithm cannot correctly detect all individual codes it would result in extra OPEX when a fault occurs. If a code does not have false detections it can be immediately identified. However, the presence of false detections will require an exhaustive search. In addition, if a large number of them is present it may involve an excessive processing time that would lead to an increase in the MDT, hence reducing customers' satisfaction.

In this context, it is desirable to have an estimation of the number of false detections when designing the monitoring system in order to obtain a trade-off between a rapid network discovery algorithm, i.e. having few false detections, and a low-cost monitoring system, i.e. low CAPEX.

Previous works as [6] and [7] deal with the implementation of the network discovery algorithm but they do not address the issue of the number of false detections. In this paper, for the first time, an analytical expression for the average number of false detections in a coding-based PON monitoring scheme is derived and the system performance in terms of false detections for different parameters is evaluated.

This work was partially supported by Consejo Nacional de Investigaciones Científicas y Técnicas CONICET, Universidad Nacional de Cuyo UNCuyo, Comisión Nacional de Energía Atómica CNEA and Sofrecom Argentina SA.

The authors are with Laboratorio de Fotónica en Microondas y Comunicaciones Ópticas, Instituto Balseiro, Bariloche 8400 (RN), Argentina.

M. P. Fernández is fellow of CONICET (e-mail: manuel.fernandez@ib.edu.ar). P. A. Costanzo Caso and L. A. Bulus Rossini are researchers of CONICET and professors at Instituto Balseiro UNCuyo (email: pcostanzo@ib.edu.ar; lbulus@ib.edu.ar).

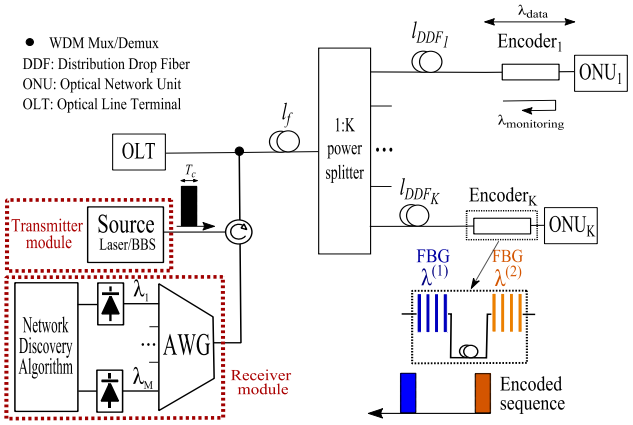

Fig. 1. Principle of the coding-based PON monitoring system.

II. PON Monitoring Scheme

A. Principle of operation

Figure 1 illustrates the proposed monitoring system. In the CO, the transmitter module sends a U-band monitoring pulse of width T_c through a feeder fiber of length l_f to the remote node. The pulse is transmitted to each drop fiber of length l_{DDFk} which is terminated by an optical encoder with a unique code. Therefore, the total distance from the CO to user-k is $l_k \equiv l_f + l_{DDFk}$. The pulse is 2D coded into two sub-pulses in both time and wavelength domains, and reflected back. In the CO, the sum of all K codes is received. The different wavelength bands are demultiplexed and photodetected. Finally, the signals are sampled and the network discovery algorithm needs to detect all individual codes.

B. Code Family

When selecting the codes, it should be noted that the requirements for a monitoring application are very distinct from that needed for data transmission; low-cost, simple fabrication and low insertion loss are mandatory requirements for encoders. In the proposed scheme, each user is assigned a code with Hamming weight $w = 2$, where the '1' chips have different wavelengths. The reason for this choice is that encoders can be fabricated with low-cost components, for example, writing two fiber Bragg gratings (FBG) with 100% reflectivity at different central wavelengths in a patch cord [8]. This type of encoders have been already successfully employed for PON monitoring applications [6].

The code corresponding to user-k is defined by the set $\{P_k, (\lambda_k^{(1)}, \lambda_k^{(2)})\}$, where P_k is the separation between the two

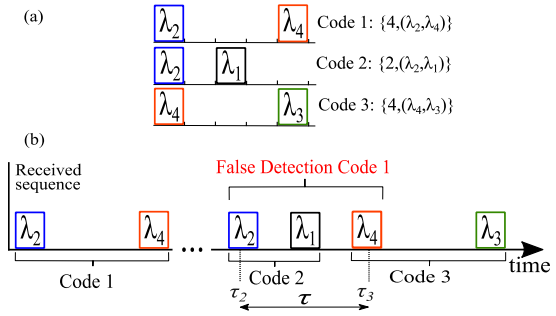

Fig. 2. Example of three codes (a) and a false detection (b).

'1' chips and ($\lambda_k^{(1)}$, $\lambda_k^{(2)}$) are its corresponding wavelengths. As an example, Fig. 2(a) shows three codes corresponding to the sets {4, (λ_2, λ_4)}, {2, (λ_2, λ_1)} and {4, (λ_4, λ_3)}.

There are M available wavelengths (λ_1, …, λ_M), with $M \geq 2$. It should be noted that the complexity and cost of the system increase with M since more components would be needed at the receiver module.

For optical orthogonal codes, one can construct a set of K codes with a maximum length $F = Kw(w-1)+1$ [9]. In our coding scheme up to $M(M-1)$ codes can have identical P by using a different pair of wavelengths. In this way, we can construct a set of K codes with a maximum length F given by

$$F \equiv \max\{P_k\} + 1 = \left\lfloor \frac{Kw(w-1)+1}{M(M-1)} \right\rfloor. \quad (1)$$

Note that the physical size of the encoders can be reduced at the expense of a more complex receiver by increasing M and/or reducing T_c. Finally, the correlation distance of a code family is defined as $l_{CD} = v_g F T_c/2$ [9]-[10], where v_g is the group velocity in the fiber.

C. Network Discovery Algorithm

The proposed algorithm can be described as follows: after being sampled, the detected sequences are hard limited in order to avoid few specific interference patterns from causing a false detection when using a correlation filter as decoder. We thus obtain a binary sequence for each wavelength band. Then, the resulting M binary sequences are decoded using a bank of correlator filters. Ideally, the output of each decoder will have an autocorrelation peak of amplitude equal to $w = 2$. However, interference between two users (i.e. the sum of their codes) may produce a sequence similar to that of the desired user. Fig. 2(b) shows a case where interference between user-2 and user-3 will cause a false detection at the output of the decoder of user-1.

A user with no false detections can be immediately identified while users with false detections will require an in-depth search. In addition, too many false detections may need an exhaustive search (e.g. a maximum likelihood sequence estimation algorithm), and a large search space would require an excessive processing time [7].

After each code is identified, the link status can be determined by soft-decoding the detected signal and evaluating the auto-correlation peak amplitude. At this stage, the system performance is evaluated with the signal-to-interference ratio (SIR), defined in [9].

III. False Detections

In this section we derive an analytical expression for the average number of false detections. Without loss of generality, we define user-1 as the desired user and the remaining $K-1$ users are potentially interfering users.

We first define a Bernoulli random variable $\Phi_{i,j} = \{0,1\}$ that takes the value '1' only if the sum of the codes of user-i and user-j generates a sequence equal to that of user-1 (i.e. it will produce a false detection). Hence, the number of false detections N_{FD} for user-1 is given by

$$N_{FD} = \sum_{i=2}^{K-1} \sum_{j=i+1}^{K} \Phi_{i,j}. \quad (2)$$

The number of false detections is a random variable that depends on the users' distribution. We define $\overline{N_{FD}}$ as the expected value of N_{FD} taken over the distances $\underline{l} = \{l_1, l_2, \ldots, l_K\}$, which we consider independent and identically distributed (i.i.d) random variables with probability density function (PDF) $p_{l_k}(l)$ that is non-zero on the interval $l = (l_f, l_f + \Delta l)$, where Δl is the maximum DDF length. Taking this into account, $\overline{N_{FD}}$ can be written as

$$\overline{N_{FD}} = \sum_{i=2}^{K-1} \sum_{j=i+1}^{K} \bar{\Phi}_{i,j} = \binom{K-1}{2} \bar{\Phi}_{2,3}\,, \quad (3)$$

where user-2 and user-3 are two arbitrary users and $\bar{\Phi}_{i,j}$ is the expected value of $\Phi_{i,j}$, or equivalently, the probability of a false detection caused by users i and j. Hence, we need to find an expression for $\bar{\Phi}_{2,3}$ to determine the value of $\overline{N_{FD}}$.

A. Received and sampled signals

As in typical incoherent OCDMA analysis, we consider chip synchronous interference and we assume a sampling rate of $1/T_c$. For mathematical convenience, we neglect noise effects since they can be reduced through appropriate averaging.

We define c_1 as a local version of the desired code-1 and c_2 and c_3 as the sampled and hard limited versions of the two interfering codes. These signals can be written as

$$\begin{aligned} c_1 &= \delta(i, \lambda_1^{(1)}) + \delta(i - P_1, \lambda_1^{(2)}) \\ c_2 &= \delta(i - \tau_2, \lambda_2^{(1)}) + \delta(i - \tau_2 - P_2, \lambda_2^{(2)}) \\ c_3 &= \delta(i - \tau_3, \lambda_3^{(1)}) + \delta(i - \tau_3 - P_3, \lambda_3^{(2)}) \end{aligned} \quad (4)$$

where the second argument in the δ function indicates the wavelength of the sampled pulse. Note that c_2 and c_3 are delayed τ_2 and τ_3 samples (chips), respectively. These delays are random variables that depend on the users' distribution and they can take any integer value on the interval $[0, \ldots, N]$, where $N = \lceil 2(l_f + \Delta l)/(T_c v_g) \rceil$. Since false detection probability is related to the distance difference between users, we define a relative delay $\tau \equiv \tau_3 - \tau_2$ whose PDF will be derived next.

B. Probability density function for the relative delay τ

The PDF for the random variable τ_k $\forall k = 1, \ldots, K$ can be obtained from the user's distance l_k as

$$p_{\tau_k}(m) = \Pr\left\{m\frac{T_c v_g}{2} < l_k \le (m+1)\frac{T_c v_g}{2}\right\} \approx \frac{T_c v_g}{2} p_{l_k}\left(m\frac{T_c v_g}{2}\right), \quad (5)$$

where $p_{\tau_k}(m)$ has been simplified as shown in the second line of Eq. (5) by assuming that $T_c v_g/2$ is sufficiently small.

The PDF for the relative delay τ can be obtained by performing the convolution of the PDFs of the random variables τ_3 and $-\tau_2$ as

$$p_\tau(n) \approx \frac{T_c v_g}{2}\int_{l_f}^{l_f+\Delta l} p_{l_3}(l) p_{-l_2}\left(n\frac{T_c v_g}{2} - l\right) dl = \frac{T_c v_g}{2} p_{l_3-l_2}\left(n\frac{T_c v_g}{2}\right), \quad (6)$$

where the result can be written in terms of p_{l_2} and p_{l_3} and n can take any integer value on the interval $[-N, \ldots, N]$. Note that the integral in Eq. (6) is the PDF of the distance difference $p_{l_3-l_2}(nT_c v_g/2)$.

C. Conditional probability of false detection given τ

The decoded sequence for the user-1 is obtained by performing the correlation between c_1 and the detected, sampled and hard limited sequences containing all codes. For two arbitrary interfering codes c_2 and c_3 it is given by

$$dec_1 = c_1 \otimes (c_2 + c_3), \quad (7)$$

where $\otimes$ denotes the correlation operator. The hard limiter will exclude some combinations of interference patterns from causing a false detection (i.e. $dec_1(i) = 2$ for some i). There is a total of eight events that produce a false detection and the events must occur simultaneously in the time and wavelength domains.

Table I shows the events that produce a false detection and the probability associated with each one. In this analysis we consider that the set $\{P_1, P_2, P_3\}$ are i.i.d random variables that follow a discrete uniform distribution $\mathrm{U}\{0, F-1\}$ and $\Pi(\mathrm{x})$ and $\Lambda(\mathrm{x})$ are the rectangular and triangular functions, respectively. Since there are M available wavelengths and there must be a double coincidence, the probability of coincidence in the wavelength domain p_λ can be shown to be $p_\lambda = 1/M^2$. By taking into account that those in Table I are mutually exclusive events, the probability of false detection caused by c_2 and c_3 can be obtained by adding the probabilities of all events. If we define $F'=F-1$, the conditional probability of false detection for a given relative delay $p_\Phi(\Phi = 1|\tau)$ is

$$p_\Phi(\Phi = 1|\tau) = \frac{p_\lambda}{F}\left[\Pi\left(\frac{\tau}{2F'}\right) + 2\Lambda\left(\frac{\tau}{2F'}\right) + \sum_{\Omega=-F'}^{F'}\frac{1}{F}\Lambda\left(\frac{\tau+\Omega}{F'}\right)\right]. \quad (8)$$

This equation is represented in Fig. 3 as a function of τ. It can be seen that a maximum value of $4p_\lambda/F$ is reached for $\tau = 0$. The probability decreases as $|\tau|$ increases: there is a sharp fall when $|\tau| = F$ and is zero when $|\tau| \ge 2F$. The relative delay $|\tau| = 2F$ corresponds to a distance difference $|l_3 - l_2| = 2l_{\mathrm{CD}}$, so only users that differ in distance by less than twice the correlation distance may cause a false detection. A pessimistic bound is given as $(4p_\lambda/F)\Pi\left(\tau/4F'\right)$, as shown with a red dashed line in Fig. 3.

TABLE I
EVENTS THAT CAUSE A FALSE DETECTION

Event		Probability
Time	Wavelength	
$\tau = P_1$	$\lambda_1^{(1)} = \lambda_2^{(1)}$ & $\lambda_1^{(2)} = \lambda_3^{(1)}$	$\frac{p_\lambda}{F}\Pi\left(\frac{\tau - \frac{F-1}{2}}{F-1}\right)$
$\tau = P_1 - P_3$	$\lambda_1^{(1)} = \lambda_2^{(1)}$ & $\lambda_1^{(2)} = \lambda_3^{(2)}$	$\frac{p_\lambda}{F}\Lambda\left(\frac{\tau}{F-1}\right)$
$\tau = P_1 + P_2$	$\lambda_1^{(1)} = \lambda_2^{(2)}$ & $\lambda_1^{(2)} = \lambda_3^{(1)}$	$\frac{p_\lambda}{F}\Lambda\left(\frac{\tau-(F-1)}{F-1}\right)$
$\tau = P_1 + P_2 - P_3$	$\lambda_1^{(1)} = \lambda_2^{(2)}$ & $\lambda_1^{(2)} = \lambda_3^{(2)}$	$\frac{p_\lambda}{F}\sum_{\Omega=0}^{F-1}\frac{1}{F}\Lambda\left(\frac{\tau+\Omega}{F-1}\right)$
$\tau = -P_1$	$\lambda_1^{(2)} = \lambda_2^{(1)}$ & $\lambda_1^{(1)} = \lambda_3^{(1)}$	$\frac{p_\lambda}{F}\Pi\left(\frac{\tau + \frac{F-1}{2}}{F-1}\right)$
$\tau = -P_1 - P_3$	$\lambda_1^{(2)} = \lambda_2^{(1)}$ & $\lambda_1^{(1)} = \lambda_3^{(2)}$	$\frac{p_\lambda}{F}\Lambda\left(\frac{\tau+(F-1)}{F-1}\right)$
$\tau = -P_1 + P_2$	$\lambda_1^{(2)} = \lambda_2^{(2)}$ & $\lambda_1^{(1)} = \lambda_3^{(1)}$	$\frac{p_\lambda}{F}\Lambda\left(\frac{\tau}{F-1}\right)$
$\tau = -P_1 + P_2 - P_3$	$\lambda_1^{(2)} = \lambda_2^{(2)}$ & $\lambda_1^{(1)} = \lambda_3^{(2)}$	$\frac{p_\lambda}{F}\sum_{\Omega=0}^{F-1}\frac{1}{F}\Lambda\left(\frac{\tau-\Omega}{F-1}\right)$

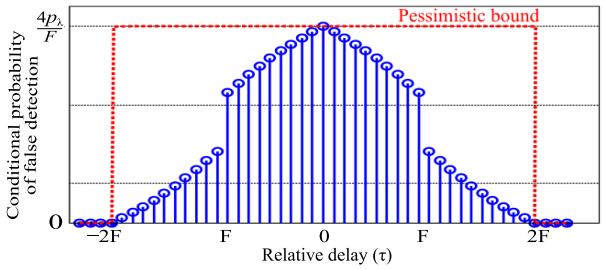

Fig. 3. Conditional probability of a false detection $p_\phi(\Phi = 1|\tau)$ versus τ.

D. Average number of false detections

Finally, the probability of false detection $\bar{\Phi}_{2,3}$ can be obtained through the law of total probability as

$$\bar{\Phi}_{2,3} = \sum_{b=-N}^{N} p_\Phi(\Phi = 1|\tau = b) p_\tau(b), \quad (9)$$

by substituting Eq. (6) and Eq. (8) into the corresponding terms in Eq. (9). For large N, the summation in Eq. (9) can be replaced by an integral. By doing $\mathrm{b} = (2l)/(T_c v_g)$, $\overline{N_{FD}}$ can be written in terms of distances. Finally, taking into account that $p_{l_3-l_2}(x)$ is zero when $|x| > \Delta l$, the average number of false detections $\overline{N_{FD}}$ can be written as

$$\overline{N_{FD}} \approx \binom{K-1}{2}\int_{-\Delta l}^{\Delta l} p_\Phi\left(\Phi = 1\left|\frac{2x}{T_c v_g}\right.\right) p_{l_3-l_2}(x) dx, \quad (10)$$

which is a valid expression for any user's geographic distribution, by properly substituting $p_{l_3-l_2}(x)$. Note that by normalizing $\overline{N_{FD}}$ by $\binom{K-1}{2}$ we obtain the probability of false detection caused by two arbitrary users. By using the pessimistic bound for the conditional probability of false

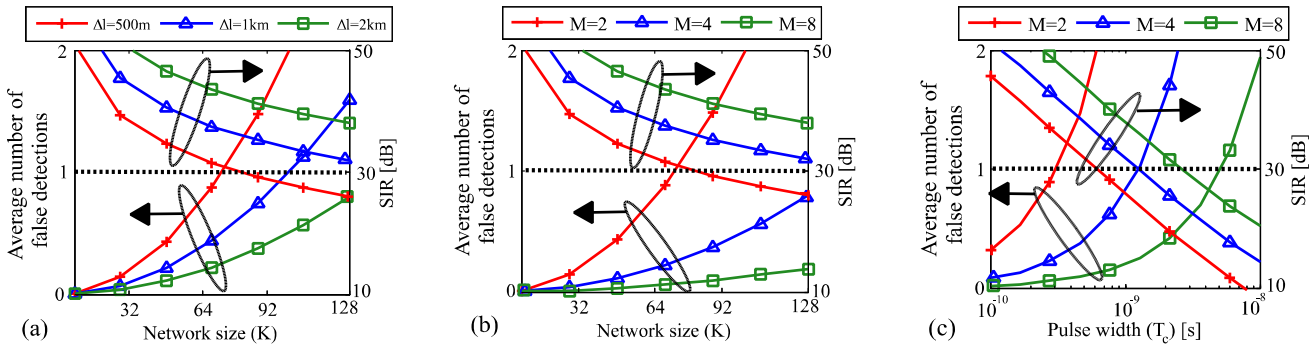

Fig. 4. $\overline{N_{FD}}$ and the SIR: versus K for different maximum DDF lengths, where $M = 2$ and $T_c = 1$ ns (a), versus K for different values of M, where $\Delta l = 500$ m and $T_c = 1$ ns (b) and versus T_c for different values of M where $\Delta l = 500$ m and $K = 128$ (c).

detection and assuming that users follow a uniform radial distribution [9] an upper bound for $\overline{N_{FD}}$ is obtained as follows:

$$\overline{N_{FD}} \leq \binom{K-1}{2} \frac{16 p_\lambda}{F} \frac{l_{CD}}{\Delta l} \left(1 - \frac{l_{CD}}{2\Delta l}\right). \quad (11)$$

IV. Results

In this section we evaluate the average number of false detections and the signal-to-interference ratio for different network and system parameters. While the SIR has impact on the false alarm probability in this type of interference-limited systems [10], when a fault occurs, a low $\overline{N_{FD}}$ is needed in order to have a rapid discovery algorithm. To this respect, we establish as a desirable design criteria to have less than one false detection per user ($\overline{N_{FD}} < 1$). In all the following analysis, we consider that users follow a uniform radial distribution.

Fig. 4(a) shows $\overline{N_{FD}}$ and the SIR versus K for different maximum DDF lengths. By using only two wavelengths and a pulse width of 1 ns, it can be seen that the monitoring system is able to support up to 64 users in a relatively high-density PON ($\Delta l = 500$ m) and more than 128 users when $\Delta l = 2$ km, while having in all cases a SIR higher than 25 dB.

The dependence of $\overline{N_{FD}}$ and the SIR on the number of wavelengths M is shown in Fig. 4(b), where it was fixed $\Delta l = 500$ m and $T_c = 1$ ns. It can be seen that $\overline{N_{FD}}$ is greatly reduced by increasing the number of used wavelengths: up to 64 users can be monitored with only $M = 2$ and more than 128 users by using $M = 4$ wavelengths. Recall that M is limited by the available bandwidth and the complexity and cost of the receiver module. In all cases we obtain a high SIR, which lead to a lower false alarm probability during the operation stage.

We finally study the dependence of $\overline{N_{FD}}$ on the system parameters in a fixed network topology in order to obtain a trade-off between cost and system performance. The use of extremely short pulses requires more expensive sources and receivers and increases the dispersion induced penalties. On the other hand, for very long pulses, encoders are bulky and impractical. To this respect, pulses on the order of nanoseconds are a practical choice. Figure 4(c) represents $\overline{N_{FD}}$ and the SIR versus T_c for different values of M when there are 128 users distributed over only 500 meters. In this case, by using $M = 2$, pulses shorter than 0.3 ns would be needed to satisfy the design criteria, while for $M = 4$, pulses up to 1 ns can be used. In both cases, a SIR around 30 dB is obtained.

V. Conclusion

We derived an analytical expression for the average number of false detections in a coding-based PON monitoring scheme. This is a useful tool for designing such a monitoring system. It gives an estimation of the number of false detections that the network discovery algorithm will have to deal with, given a network topology (K, Δl) and the monitoring system parameters (M, T_c). We showed that a low-cost scheme, which implies feasible system parameters such as $M = 2$ and $T_c = 1$ ns, can support the maximum split-ratio defined for widely-deployed PON standards such as GPON: 128 users in moderate-density PONs and up to 64 users in high-density PONs. A similar analysis could be made to obtain $\overline{N_{FD}}$ for other coding-based monitoring schemes by just extending the presented procedure.

References

[1] M. M. Rad et al. "Passive optical network monitoring: Challenges and requirements," *IEEE Commun. Mag*., vol.49, no.2, pp.45–52, Feb. 2011.

[2] H. Fathallah, M. M. Rad and L. A. Rusch, "PON Monitoring: Periodic Encoders With Low Capital and Operational Cost," *IEEE Photonics Technol. Lett.*, vol. 20, no. 24, pp. 2039-2041, Dec. 2008.

[3] M. M. Rad et al. "A Novel Pulse-Positioned Coding Scheme for Fiber Fault Monitoring of a PON," *IEEE Communications Letters*, vol. 15, no. 9, pp. 1007-1009, September 2011..

[4] M. P. Fernández, P. A. Costanzo Caso and L. A. Bulus Rossini, "Design and performance evalauation of an optical coding scheme for PON monitoring," in *XVI Workshop on Information Processing and Control*, Cordoba, 2015.

[5] M. P. Fernández, P. A. Costanzo Caso and L. A. Bulus Rossini "Efectos de backscattering, dispersión, coherencia y ruido en un sistema de monitoreo de redes PON". in *IEEE Biennial Congr. of Argentina (ARGENCON)*, Buenos Aires, 2016

[6] X. Zhou, F. Zhang and X. Sun, "Centralized PON Monitoring Scheme Based on Optical Coding," *IEEE Photonics Technol. Lett.*, vol. 25, no. 9, pp. 795-797, May 2013.

[7] M. M. Rad, et al. "Computationally Efficient Monitoring of PON Fiber Link Quality Using Periodic Coding," *IEEE/OSA J. Opt. Commun. Netw.*, vol. 3, no. 1, pp. 77-86, January 2011.

[8] H. Fathallah and M. Esmail. "Performance evaluation of special optical coding techniques appropriate for physical layer monitoring of access and metro optical networks," *Photon. Netw. Commun.*, vol 30, no.2, pp.223-233, 2015.

[9] M. M. Rad et al. "Fiber fault PON monitoring using optical coding: Effects of customer geographic distribution," IEEE Trans. Commun., vol. 58, no. 4, pp. 1172–1181, Apr. 2010.

[10] M. M. Rad et al. "Performance analysis of fiber fault PON monitoring using optical coding: SNR, SNIR, and false-alarm probability," *IEEE Trans. Commun.*, vol.58, pp. 1182-1192, April 2010.